

Investigating surfaces, geometry and degree of fusion of tracks printed using fused deposition modelling to optimise process parameters for polymeric materials at meso-scale

Fredrick Mwanja, Maina Maringa, Joseph Nsengimana and Jacobus Gert van der Walt
Department of Mechanical and Mechatronic Engineering, Central University of Technology Free State,
Bloemfontein, South Africa

Abstract

Purpose – The current analysis was conducted to investigate the quality of surfaces and geometry of tracks printed using PolyMide™ CoPA, Polymax™ PC and PolyMide™ PA6-CF materials through fused deposition modelling (FDM). This study also examined the degree of fusion of adjacent filaments (tracks) to approximate the optimal process parameters of the three materials.

Design/methodology/approach – Images of fused adjacent filaments were acquired using scanning electron microscopy (SEM), after which, they were analysed using Image J Software and Minitab Software to determine the optimal process parameters.

Findings – The optimal process parameters for PolyMide™ CoPA are 0.25 mm, 40 mm/s, –0.10 mm, 255°C and 0.50 mm for layer thickness, printing speed, hatch spacing, extrusion temperature and extrusion width, respectively. It was also concluded that the optimal process parameters for Polymax™ PC are 0.30 mm, 40 mm/s, 0.00 mm, 260°C and 0.6 mm for layer thickness, printing speed, hatch spacing, extrusion temperature and extrusion width, respectively.

Research limitations/implications – It was difficult to separate tracks printed using PolyMide™ PA6-CF from the support structure, making it impossible to examine and determine their degree of fusion using SEM.

Social implications – The study provides more knowledge on FDM, which is one of the leading additive manufacturing technology for polymers. The information provided in this study helps in continued uptake of the technique, which can help create job opportunities, especially among the youth and young engineers.

Originality/value – This study proposes a new and a more accurate method for optimising process parameters of FDM at meso-scale level.

Keywords Fused deposition modelling, Polymeric materials, Process parameters, Filaments, Degree of fusion of tracks, Optimisation

Paper type Research paper

1. Introduction

Fused deposition modelling (FDM) involves extruding semi-molten filaments to form a layer consisting of a pre-determined pattern of fused filaments (tracks, roads, beads, strands or rasters) (Li *et al.*, 2002). The process continues where layer upon layer is deposited, resulting in formation of three-dimensional (3D) parts, as illustrated in Figure 1. Bonding of adjacent filaments can be considered a first step for developing 3D components using FDM.

Gao *et al.* (2021) noted that fusion of adjacent filaments is similar to welding of films that involves three steps: surface contact, neck growth and molecular diffusion and cross-linking across the interface of filaments, as summarised in Figure 2.

The current issue and full text archive of this journal is available on Emerald Insight at: <https://www.emerald.com/insight/1355-2546.htm>



Rapid Prototyping Journal
30/11 (2024) 159–172
Emerald Publishing Limited [ISSN 1355-2546]
[DOI 10.1108/RPJ-02-2024-0069]

© Fredrick Mwanja, Maina Maringa, Joseph Nsengimana and Jacobus Gert van der Walt. Published by Emerald Publishing Limited. This article is published under the Creative Commons Attribution (CC BY 4.0) licence. Anyone may reproduce, distribute, translate and create derivative works of this article (for both commercial and non-commercial purposes), subject to full attribution to the original publication and authors. The full terms of this licence may be seen at <http://creativecommons.org/licenses/by/4.0/legalcode>

The authors would like to thank Product Development Technology Station at the Central University of Technology (CUT), Free State, for their assistance with the printing of the filament-parts using FDM. Special gratitude is also extended to the Department of Geology, University of the Free State, South Africa, for their assistance with the SEM experiments.

Funding: This research was funded by CPAM programme (Collaborative Program in Additive Manufacturing), grant number CSIRNLC-CPAM-18-MOA-CUT-03. The APC was funded by CPAM.

Data availability statement: All the information will be available on request.

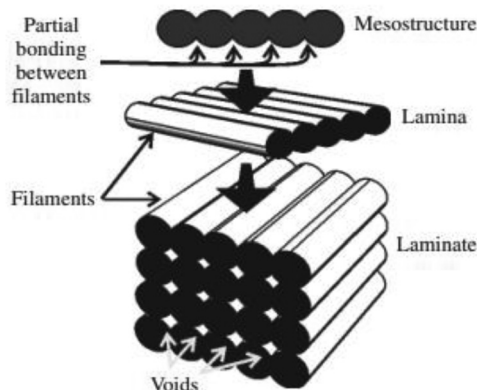
Conflicts of interest: The authors declare no conflict of interest.

Received 7 February 2024

Revised 23 April 2024

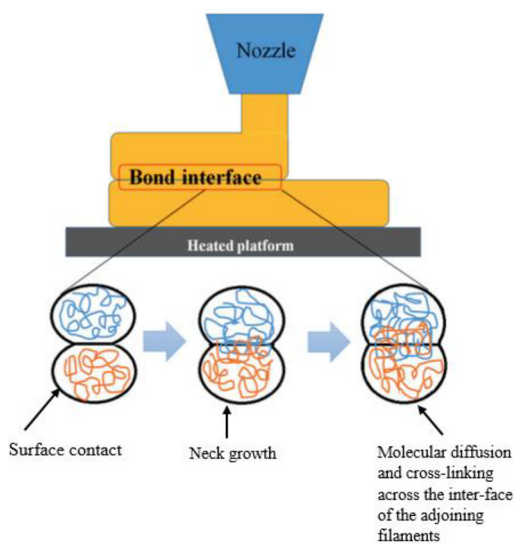
Accepted 24 May 2024

Figure 1 Schematic representation of the process of developing parts in FDM



Source: Figure sourced from Bellehumeur *et al.* (2004)

Figure 2 The steps of bond formation between adjoining filaments



Source: Figure sourced from Gao *et al.* (2021)

The quality of bonds formed between adjacent filaments and layers is very crucial as it determines the physical and mechanical properties of the finished products (Krajangsawadi *et al.*, 2021). Furthermore, quantifying the degree of fusion and bond property between adjacent filaments is an essential step to determine mechanical characteristics of parts printed using FDM (Tao *et al.*, 2021). Hence, the need for investigation of bond formation to provide crucial information on FDM at the meso-structure level.

Despite being one of the most popular AM technologies, FDM is a complex process that is influenced by a myriad of parameters (Naveed, 2021). Mwema and Akinlabi (2020) broadly classified these parameters into machine or materials aspects, which include factors summarised in Figure 3.

The qualities of parts printed using FDM are subject to various process parameters, such as infill density, infill patterns, extrusion temperature, bed temperature, layer thickness, nozzle diameter, raster angle and build orientation (Syrlybayev *et al.*, 2021). Syrlybayev *et al.* (2021) noted that the most crucial requirements, for finished parts, include mechanical strength, surface roughness and dimensional accuracy. The authors added that the extent of inter-layer bonding, intra-layer bonding and neck size determines the mechanical properties of printed components. Tao *et al.* (2021) mentioned that FDM is affected by the presence of voids and poor layer-to-layer fusion, which results in weak components with anisotropic characteristics.

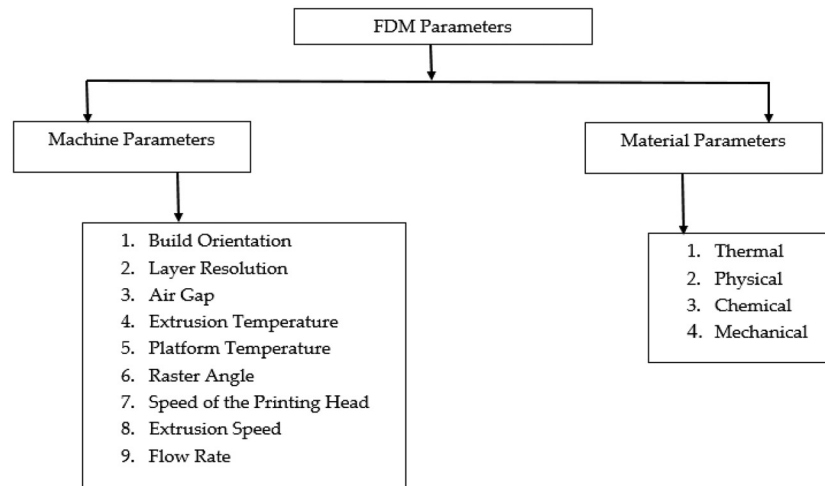
Unlike powder bed fusion for polymers, where the most crucial process parameters that affect powder particle fusion have been identified, information is still missing to link different FDM process parameters to the fusion of adjacent filaments (Xia *et al.*, 2019). Therefore, it is imperative to investigate neck formation for two adjacent filaments to gain more insights into FDM for different polymers, and to determine how different process parameters influence intra-layer bonding and neck size.

FDM is among the most popular additive manufacturing technologies for polymers (Ismail *et al.*, 2022). As a result, numerous commercial and research materials, such as acrylonitrile-butadiene-styrene (ABS), poly-lactic acid (PLA), nylon (PA), polypropylene (PP), polycarbonate (PC), polyethylene terephthalate, thermoplastic polyurethane and polyethylene (PE) have been developed over the years for use in FDM (Patel *et al.*, 2022). However, it is challenging to print some of the available polymeric materials because FDM is a multifactorial process, making it difficult to establish the most optimum conditions (Kristiawan *et al.*, 2021). Considerable research has been undertaken to optimise the process parameters for different polymeric materials used in FDM to ensure a successful process and final products of high quality (Kristiawan *et al.*, 2021). However, few studies have focused on the optimisation of these process parameters at the meso-structure level, despite bond formation (fusion between adjacent filaments) being a crucial aspect of FDM because it affects the physical and mechanical properties of printed components (Xia *et al.*, 2019; Xia *et al.*, 2023). The current study investigated the surfaces and geometry of adjacent filaments (tracks) printed using PolyMide™ CoPA, Polymax™ PC and PolyMide™ PA6-CF. The study was also undertaken to examine the degree of fusion between filaments printed using the three commercial materials to establish the optimal process parameters for the materials.

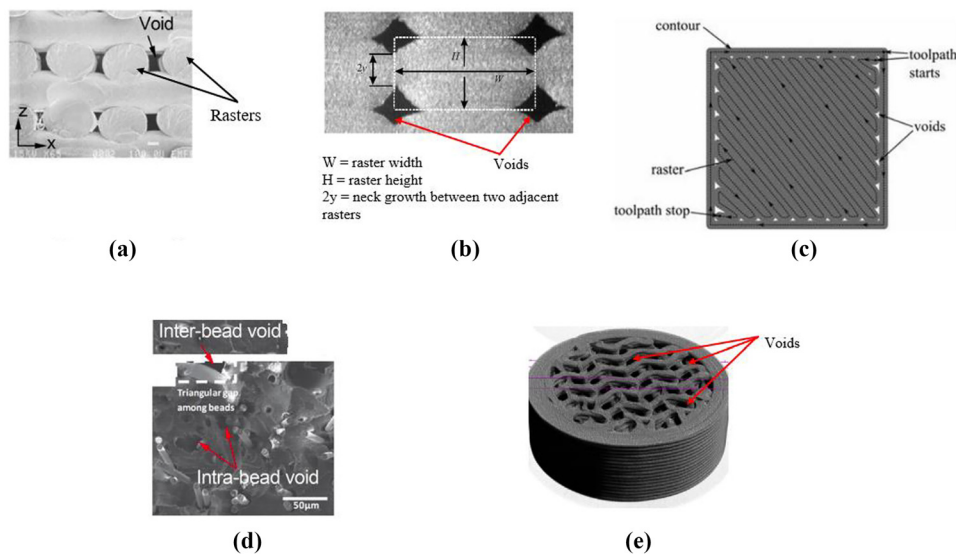
2. Literature review

2.1 Types of voids present in parts printed using fused deposition modelling

Components developed using FDM are most likely to contain either of the following voids: raster gap, partial neck growth, sub-perimeter, intra-bead or infill (Tao *et al.*, 2021). Figure 4 summarises the different types of voids common in parts printed using FDM.

Figure 3 Key machine parameters and material properties influencing the FDM process

Source: Figure sourced from Mwema and Akinlabi (2020)

Figure 4 Types of voids common in parts printed using FDM

Notes: (a) Raster gap voids; (b) partial neck growth voids (Inter-bead voids); (c) sub-perimeter voids; (d) intra-bead voids; (e) infill voids

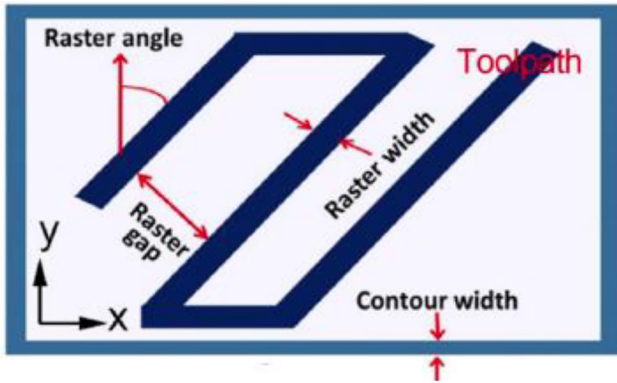
Source: Figure sourced from Tao *et al.* (2021)

A typical layer-part printed using FDM consists of a contour (shell) and rasters, as illustrated in Figure 5. Raster gap voids are formed by the spaces between adjoining filaments [Figure 4(a)]. The raster gaps can be controlled by adjusting the values of the air gap (raster gap).

The sub-perimeter voids are gaps at turning points for the filaments on the contours [Figure 4(c)]. Intra-bead voids are common in parts developed using composite materials, and occur within a bead, probably due to differing material properties [Figure 4(d)]. Infill voids are normally part of a design specification, and they are regulated through process parameters, such as infill patterns or infill density [Figure 4(e)]. Finally,

partial neck growth voids are formed due to incomplete intra-layer and inter-layer bonding, as illustrated in Figure 4(b). Partial neck growth are the main contributors of voids in parts printed using FDM, and they can be avoided through 100% fusion of adjacent filaments, but this is not practically achievable. The presence of voids reduces mechanical properties of parts printed using FDM (Krajangsawadi *et al.*, 2021). Therefore, voids should be averted. However, this might not be achievable because parts created using FDM are most likely to contain voids. It leaves a research gap to investigate the extent to which different process parameters and material properties affect neck formation, which is the focus of this study.

Figure 5 Schematic representation of a typical layer-part



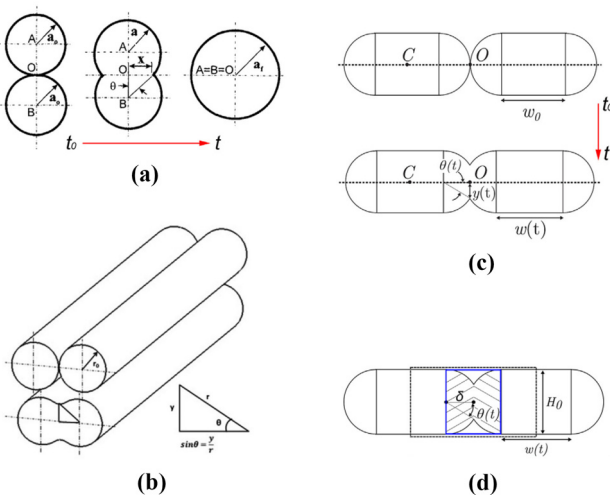
Source: Figure sourced from Tao et al. (2021)

2.2 Modelling of neck growth

The quality of fusion of adjoining filaments is imperative during the FDM process as it determines the mechanical integrity of a printed part (Gao et al., 2021; Ahmad et al., 2022). Gurralla and Regalla (2014) further alluded that the strength of parts printed using FDM is majorly dependent on the intra-layer bonding, inter-layer fusion and level of neck growth between filaments. According to Vanaei et al. (2021), bonding locations are points of failure when a component printed using FDM is subjected to external pressure.

Different models have been developed to describe neck growth and formation of partial neck growth voids. Early models were based on the fusion of two Newtonian fluid droplets, as represented in Figure 6(a) (Tao et al., 2021). The models assume that the droplets are identical to each other with radii of a_0 . The droplets coalesce after time (t), forming a resultant sphere with radius a_f . Figure 6(b) represents intra- and inter-layer bonding of cylindrical filaments in FDM.

Figure 6 Schematic representation of neck growth evolution for two spherical droplets (a), intra- and inter-layer bonding of filaments in FDM (b), and cylindrical filaments (c, d)



Source: Figure sourced from Tao et al. (2021)

Gurralla and Regalla (2014) and Frenkel (1945) developed models to describe neck growth evolution of cylindrical filaments with respect to time and viscous sintering, as illustrated by equations (1) and (2), respectively. Bhalodi et al. (2019) also developed mathematical models to relate temperature and the degree of fusion between two adjacent filaments, as summarised by equations (3) and (4):

$$\frac{d\theta}{dt} = \frac{\Gamma}{r_0 \eta} \left[\frac{2^{-\frac{5}{3}} \cos \theta \sin \theta (2 - \cos \theta)^{\frac{1}{3}}}{(1 - \cos \theta)(1 + \cos \theta)^{\frac{1}{3}}} \right] \quad (1)$$

$$\dot{\theta} = \frac{d\theta}{dt} = \frac{\Gamma}{\sqrt[3]{\pi r_0 \eta}} \left[\frac{[(\pi - \theta) \cos \theta + \sin \theta][\pi - \theta + \sin \theta \cos \theta]^{\frac{1}{2}}}{(\pi - \theta)^2 \sin^2 \theta} \right] \quad (2)$$

$$\frac{d\theta}{dT} = - \frac{\Gamma}{m v r_0 \eta (T - T_{\infty})} \left[\frac{2^{-\frac{5}{3}} \cos \theta \sin \theta (2 - \cos \theta)^{\frac{1}{3}}}{(1 - \cos \theta)(1 + \cos \theta)^{\frac{1}{3}}} \right] \quad (3)$$

$$\frac{d\theta}{dT} = - \frac{\Gamma}{\sqrt[3]{\pi m v r_0 \eta} (T - T_{\infty})} \left[\frac{[(\pi - \theta) \cos \theta + \sin \theta][\pi - \theta + \sin \theta \cos \theta]^{\frac{1}{2}}}{(\pi - \theta)^2 \sin^2 \theta} \right] \quad (4)$$

where:

- θ = intersection angle between the filaments ($^{\circ}$);
- $\dot{\theta}$ = the rate of change of the intersection angle of the neck formed, with respect to fusion time;
- Γ = coefficient of surface tension;
- r_0 = initial radius of a filament (m);
- η = viscosity of the melt of a filament ($kg \cdot m^{-1} \cdot s^{-1}$);
- t = sintering time (s);
- m = mass of the filament (kg);
- v = velocity of nozzle (m/s);
- T = temperature at the interface of adjacent filaments ($^{\circ}C$); and
- T_{∞} = temperature of the build platform ($^{\circ}C$).

Figures 6(c) and 6(d), provide an actual representation of bonding of two adjacent filaments. Tao et al. (2021) proposed a mathematical model to describe radial width of the growth of the neck with the time [based on Figures 6(b–d)], presented here as equation (5):

$$y(t) = \frac{H_0}{2} \sin \theta(t) \quad (5)$$

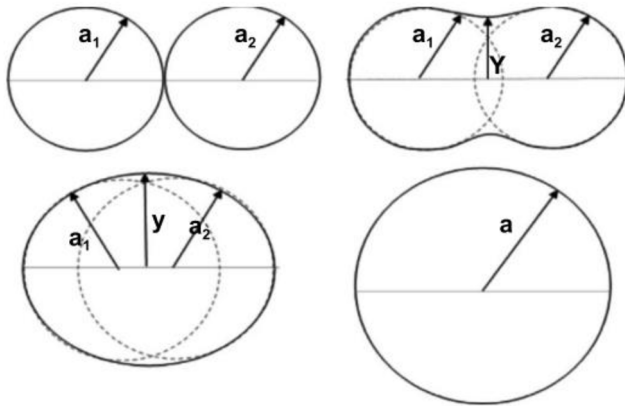
where:

- $y(t)$ = radial width of neck growth (m);
- H_0 = raster height (m); and
- $\theta(t)$ = intersection angle = $\sin^{-1} \frac{y}{r} = \tan^{-1} \frac{y}{\delta}$.

Han et al. (2022) also used the Frenkel-Eshelby model to describe the fusion of sintered particles in polymer laser sintering (PLS), resulting in formation of a melt that solidified to form a three-dimensional component. The model considers two adjacent particles that fuse together with increasing temperature as illustrated in Figure 7, where a_1 and a_2 are radii of two adjacent particles, y is the radius of the neck and a is the radius of resulting spherical melt.

In the current study, the Frenkel–Eshelby model could be used to explain the fusion of two adjacent threads despite the fact that FDM considers films as opposed to PLS, where powder particles are considered. One of the first models proposed by Frenkel that

Figure 7 Schematic representation of the Frenkel–Eshelby model, which is used to describe fusion of two adjacent particles in PLS



Source: Figure sourced from Han *et al.* (2022)

described coalescence of particles driven by viscous flow (Lupone *et al.*, 2021) was modified. Equation (6) represents the Frenkel’s model which was modified in the present work due its simplicity and ease of measuring the length of the neck between two adjacent filaments from images obtained using scanning electron microscopy (SEM):

$$\left(\frac{y}{a_{12}}\right)^2 = \frac{3\sigma t}{2a\eta_0} \quad (6)$$

where:

- y = length of growing neck between two filaments (m);
- a_{12} = initial radii of two adjacent filaments (m);
- σ = surface tension of the material (N/m);
- t = time (s);
- a = radius of resulting fused track (m); and
- η_0 = viscosity of the material ($kg.m^{-1}.s^{-1}$).

Mwanja *et al.* (2023) considered that the ratio of the total height (h) of the neck to the diameter (d) of two adjacent filaments after fusion and cooling (h/d) is directly proportional to the degree of fusion [equation (7)]. The study considered that higher values represent better coalescence of filaments, which also represents better process parameters for a particular material. Figure 8 shows the total height of the neck and the diameter of two adjacent filaments after fusion and cooling:

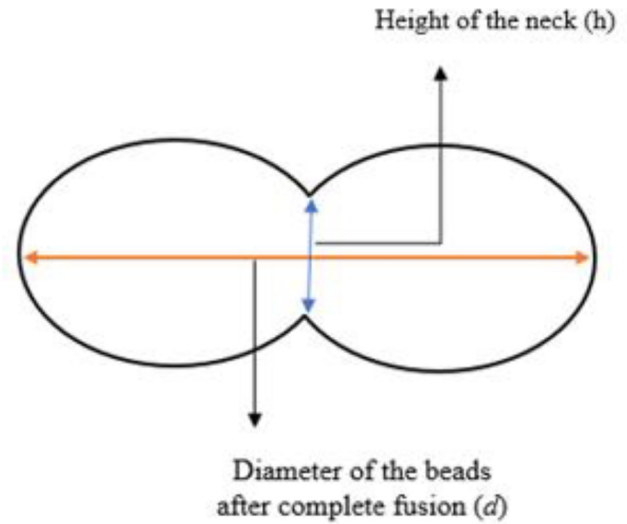
$$\delta_f = \frac{h}{d} \quad (7)$$

Where:

- δ_f = degree of fusion between adjoining filaments;
- h = total height of the neck (m); and
- d = diameter of two adjacent filaments after fusion and cooling.

In the current study, the degree of fusion of two adjacent tracks printed using FDM was investigated. This research aims to act as a starting point for studying degrees of fusion of tracks to establish an analytical model involving crucial process parameters used for FDM.

Figure 8 Schematic representation of the total height of the neck and the diameter of two adjacent filaments after fusion and cooling



Source: Figure sourced from Mwanja *et al.* (2023)

3. Materials and methods

3.1 Printing equipment

The specimens were built using an FDM desktop UP Mini 2 ES Printer (Figure 9).

According to the manufacturers of the equipment, the printer can be used for educational, domestic and industrial purposes. The specifications of the printing machine are outlined in Table 1.

3.2 Materials used

Two commercial polymeric filaments (PolyMide™ CoPA and Polymax™ PC, as well as the polymer composite PolyMide™ PA6-CF) from the supplier, Polymaker, were used in this

Figure 9 The UP Mini 2 ES Printer that was used in this study



Source: Figure by authors

Table 1 Specifications of up mini 2 ES mini printer

#	Description and parameter	Specification
1	Printing technology	Melted extrusion modelling (MEM)
2	Extruder	1
3	Nozzle diameter	0.4 mm
4	Maximum extruder temperature	299°C
5	Maximum extruder travel speed	200 mm/sec
6	Accuracy in X, Y and Z directions	5 microns
7	Build volume	120 × 120 × 120 mm ³
8	Accuracy of printed parts	± 0.1 /100 mm
9	Layer resolutions	0.15/0.2/0.25/0.3/0.35 mm
10	Maximum temperature of the build plate	70°C
11	Recommended filament materials	ABS, PLA, TPU and others
12	Filament diameter	1.75 mm
13	Software	UP Studio version 2.5 or above
14	Supported operating system	Windows 7 or higher (32 or 64 bits) Mac OS 10.10
15	Hardware	OpenGL 2.0 with at least 4GB of RAM

Source: Table by authors

study. PolyMide™ CoPA is a copolymer consisting of nylon 6 (PA6) and nylon 6.6 (PA6.6). According to the supplier, the material has excellent strength, toughness and maximum operating temperature of 180°C. It is also suitable for printing because of limited warping. Polymax™ PC is an engineered type of polycarbonate (PC) with good printing qualities, excellent strength, toughness and resistance to heat, as specified by the supplier. The suppliers suggest that the material is suitable for a wide range of engineering applications and can withstand temperatures up to 113°C. PolyMide™ PA6-CF is a carbon fibre-reinforced PA6. According to the supplier, the carbon fibre improves the stiffness, strength, layer adhesion and heat resistance of the parent matrix. The printing conditions specified by the supplier for the three materials, are summarised in [Table 2](#).

3.3 Printing process

A simple parameter-printing matrix was considered for PolyMide™ PA6-CF at the onset, where one of the parameters shown in [Table 3](#) was varied, while the others were held constant. [Table 3](#) is a summary of the parameter-printing matrix considered for fabricating test specimens using PolyMide™ PA6-CF.

The authors used the Taguchi method to develop a matrix for the printing parameters for PolyMide™ CoPA and Polymax™ PC. Five process-parameters [layer thickness, printing speed, hatch spacing (air gap), extrusion temperature and extrusion width] with four levels were considered, as

summarised in [Table 4](#). [Table 5](#) is an outline of an L16 orthogonal array used in this analysis, while [Table 6](#) is the matrix considered for the two materials. 14 samples were printed using Polymax™ PC up to run 14 as shown in [Tables 5](#) and [6](#). For the outlined process parameters, 16 samples were fabricated using PolyMide™ CoPA.

It was evident that there was a correlation between layer thickness and the extrusion width. For instance, the software displayed an error when a layer thickness of a value more than 0.25 mm was used for an extrusion width of 0.7 mm. In addition, for runs 8, 10 and 15, extrusion widths started at 0.35, 0.38 and 0.40 mm. Hence, the printing schedule had to be adjusted to accommodate these requirements of the software.

The supplier recommends annealing of PolyMide™ CoPA at 80°C for six hours because printed parts do not reach full crystallisation after printing. The suppliers further state that the material should also be dried for six hours at 100°C, in case it absorbed moisture. The suppliers observe that Polymax™ PC can be annealed at 90°C for two hours to release internal stresses that encourage development of micro-cracks. If the parts absorbed moisture, they can be dried at 75°C for two hours. It is recommended by the suppliers that PolyMide™ PA6-CF on the other hand, can be annealed at 80°C for six hours to ensure full crystallisation of the printed parts. Moreover, the material can be dried at 100°C for eight hours, in case the printed parts absorbed moisture. The main reasons for annealing of printed parts are to minimise porosity, reduce the degree of crystallinity and relief residual stresses in the parts.

Table 2 Recommended printing parameters

#	Printing parameters	PolyMide™ CoPA	Polymax™ PC	PolyMide™ PA6-CF
1	Printing temperature (°C)	250–270	250–270	280–300
2	Bed temperature (°C)	25–50	90–105	25–50
3	Printing speed (mm/s)		30–50	
4	Fan		Off	

Source: Table by authors

Table 3 Parameter matrix for test specimens printed in PolyMide™ PA6-CF

Layer thickness (mm)	Infill density (%)	Printing speed (mm/s)	Extrusion width (mm)	Air gap (mm)	Extrusion temperature (°C)
<i>Printing matrix with variation of the layer thickness</i>					
0.05	99	45	0.58	0	245
0.20	99	45	0.58	0	245
0.25	99	45	0.58	0	245
0.30	99	45	0.58	0	245
0.35	99	45	0.58	0	245
<i>Printing matrix with variation of the infill density</i>					
0.20	15	45	0.58	0	245
0.20	20	45	0.58	0	245
0.20	65	45	0.58	0	245
0.20	80	45	0.58	0	245
0.20	99	45	0.58	0	245
<i>Printing matrix with variation of the printing speed</i>					
0.20	99	35	0.58	0	245
0.20	99	40	0.58	0	245
0.20	99	45	0.58	0	245
0.20	99	55	0.58	0	245
0.20	99	60	0.58	0	245
<i>Printing matrix with variation of the air gap</i>					
0.20	99	45	0.58	−0.10	245
0.20	99	45	0.58	−0.05	245
0.20	99	45	0.58	0.00	245
0.20	99	45	0.58	+0.05	245
0.20	99	45	0.58	+0.01	245
<i>Printing matrix with variation of the extrusion temperature</i>					
0.20	99	45	0.58	0	215
0.20	99	45	0.58	0	225
0.20	99	45	0.58	0	245
0.20	99	45	0.58	0	255
0.20	99	45	0.58	0	260

Source: Table by authors

Table 4 Process parameters and levels for printing test specimens in PolyMide™ CoPA and Polymax™ PC

#	Process parameter	Level 1	Levels of each process parameter			Level 4
			Level 2	Level 3	Level 4	
1	Layer thickness (mm)	0.15	0.2	0.25	0.30	
2	Printing speed (mm/s)	30	35	40	50	
3	Hatch spacing (mm)	−0.10	0.00	0.10	0.15	
4	Extrusion temperature (°C)	250	255	260	270	
5	Extrusion width (mm)	0.30	0.40	0.50	0.60	

Source: Table by authors

However, these post-processes were not undertaken in this study, and the specimens were analysed in the as-built state, because the study was focused on the degree of fusion of adjoining built filaments that is not subject to either of these three factors, unlike the case for three-dimensional parts. The filaments were also printed in their as-received state because they were delivered in sealed bags which prevented the absorption of moisture.

Double tracks were printed on top of a support structure, as shown in [Figure 10](#).

Different process parameters, specified in [Tables 3](#) and [6](#) were considered for different test specimens. Upon completion of printing, the samples were allowed to cool to room temperature and then placed in air-tight bags to prevent them from absorbing moisture. The top surface of the tracks printed using the three materials were examined using a SEM to assess

Table 5 L16 Orthogonal array

Run#	Layer thickness	Printing speed	Hatch spacing	Extrusion temperature	Extrusion width
1	1	1	1	1	1
2	1	2	2	2	2
3	1	3	3	3	3
4	1	4	4	4	4
5	2	1	2	3	4
6	2	2	1	4	3
7	2	3	4	1	2
8	2	4	3	2	1
9	3	1	3	4	2
10	3	2	4	3	1
11	3	3	1	2	4
12	3	4	2	1	3
13	4	1	4	2	3
14	4	2	3	1	4
15	4	3	2	4	1
16	4	4	1	3	2

Source: Table by authors

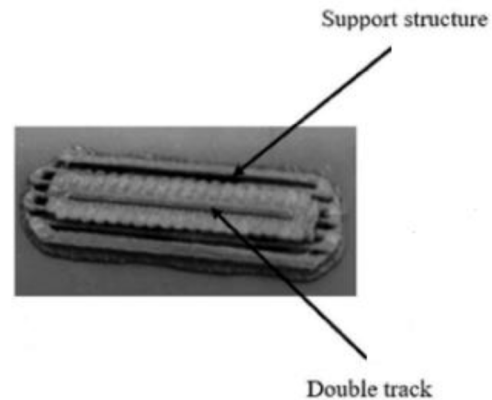
Table 6 Process-parameter matrix for printing test specimens in PolyMide™ CoPA and Polymax™ PC

Run#	Layer thickness (mm)	Printing speed (mm/s)	Hatch spacing (mm)	Extrusion temperature (°C)	Extrusion width (mm)
1	0.15	30	-0.10	250	0.30
2	0.15	35	0.00	255	0.40
3	0.15	40	0.10	260	0.50
4	0.15	50	0.15	270	0.60
5	0.20	30	0.00	260	0.60
6	0.20	35	-0.10	270	0.50
7	0.20	40	0.15	250	0.40
8	0.20	50	0.10	255	0.35
9	0.25	30	0.10	270	0.40
10	0.25	35	0.15	260	0.38
11	0.25	40	-0.10	255	0.60
12	0.25	50	0.00	250	0.50
13	0.30	30	0.15	255	0.50
14	0.30	35	0.10	250	0.60
15	0.30	40	0.00	270	0.40
16	0.30	50	-0.10	260	0.40

Source: Table by authors

the surface roughness, as well as any other irregularities. Afterwards, the tracks were cut right through the diameter using a razor blade, and the cut surfaces then assessed using a SEM to inspect the geometry of the cross-sections. The images were analysed using (*ImageJ 1.53k; Java 1.8.0_172 [64-bit]*) to measure the total height (h) of the neck and the diameter (d) of two adjacent filaments after fusion and cooling. The degree of fusion for tracks, printed at different process parameters, were quantified using equation (7) and the data obtained evaluated using Minitab statistical software to determine the optimal process parameters for the different materials.

Figure 10 A sample of a fabricated test specimen with the support structure and dual tracks



Source: Figure by authors

4. Results and discussion

4.1 Top surfaces of tracks printed using PolyMide™ CoPA, Polymax™ PC and PolyMide™ PA6-CF

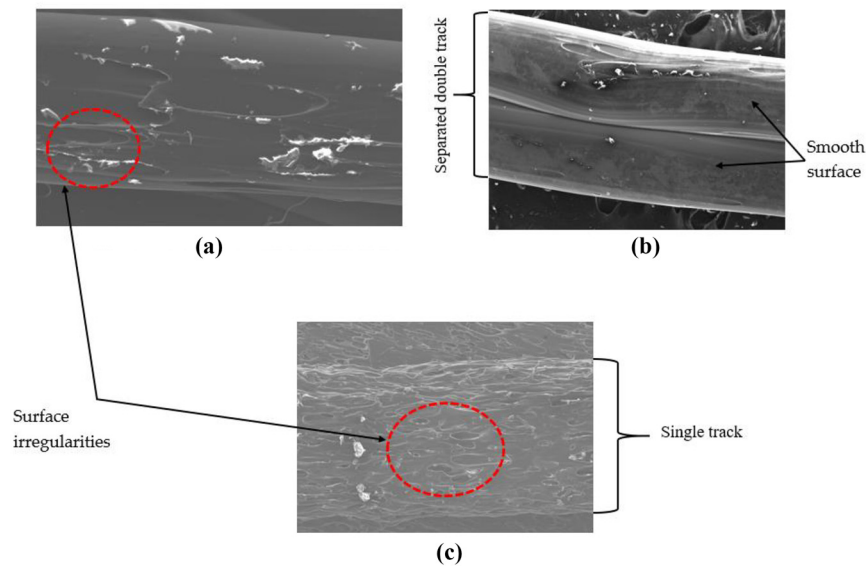
Figure 11 (Magnification X110) shows the top surface of tracks printed using PolyMide™ CoPA, Polymax™ PC and PolyMide™ PA6-CF for process parameters suggested as optimal from this analysis.

It is essential to establish the surface roughness of components printed using FDM, to ensure that they meet the requirements of tolerance and roughness, as was noted by [Boschetto et al. \(2016\)](#). A visual inspection of the printed parts shows that PolyMide™ PA6-CF had more surface irregularities (roughness) as compared to tracks printed using PolyMide™ CoPA and Polymax™ PC. This is supported by observations of the images in the foregoing figure. Parts fabricated using Polymax™ PC appeared to have the smoothest surface for all the three materials used, as is evident in [Figure 11](#). Assuming that the surface roughness of the printed tracks reflects the surface roughness of finished parts, it can be deduced that for the three materials, Polymax™ PC is the best material suitable for FDM printing, followed by PolyMide™ CoPA, for applications that require a smooth surface. This foregoing analysis suggests that PolyMide™ PA6-CF will present challenges when printed using FDM, for applications requiring smooth surfaces. This is because of notable surface roughness, as represented by the considerable irregularities on the surfaces on the tracks.

Notable research has been undertaken to investigate how different process parameters, such as layer thickness, spreading speed and raster angle, affect surface roughness of parts printed using FDM ([Sukindar et al., 2024](#); [Bintara et al., 2021](#); [Alsoufi and Elsayed, 2018](#)). However, few studies have focused on the impacts of different feedstock materials on surface roughness of printed parts. The current study, illustrates that the source of printing material will affect the surface roughness of components printed using FDM.

4.2 Geometry of the tracks printed using PolyMide™ CoPA, Polymax™ PC and PolyMide™ PA6-CF

Figure 12 shows that parts printed using Polymax™ PC and PolyMide™ CoPA have double tracks that were not fully

Figure 11 Top surfaces of tracks printed using PolyMide™ CoPA, Polymax™ PC, and PolyMide™ PA6-CF

Notes: (a) Tracks printed using polyimide™ CoPA; (b) tracks printed using polymax™ PC
(c) tracks printed using polyimide™ PA6-CF

Source: Figure by authors

fused, as opposed to tracks fabricated using PolyMide™ PA6-CF. It can be assumed by this, that parts printed using PolyMide™ PA6-CF are denser compared to parts built using Polymax™ PC and PolyMide™ CoPA because the former material results in better fusion of filaments, which can be seen through visual inspection. On the other hand, it was difficult to remove tracks printed using PolyMide™ PA6-CF from the support structure because the tracks fused with the support structure to form a single entity as illustrated in Figure 12(a). Parts printed from materials that are suitable for the FDM process should be easy to remove from the support structure to prevent damaging the components (Joseph *et al.*, 2023). The tracks printed using PolyMide™ CoPA also fused with the support structure, but the outline of the track was visible, thus making it possible to investigate the degree of fusion of the tracks, while still attached to the support structure [Figure 12(b)]. The filaments printed using Polymax™ PC were easy to remove from the support structure [Figure 12(c)], thus allowing the inspection of the level of fusion of the tracks separately from the support structure. Therefore, this study only considered bond formation and degree of fusion for tracks printed using PolyMide™ CoPA and Polymax™ PC.

4.3 Bond formation and degree of fusion of filaments printed using PolyMide™ CoPA and Polymax™ PC

Numerous process parameter optimisation studies have been undertaken, but most of them have focused on ABS, PLA and PC (Dey and Yodo, 2019). The current study optimises process-parameters for two new commercial materials (PolyMide™ CoPA, Polymax™ PC). The obtained results were analysed using Minitab software to determine the optimum process parameters of layer thickness, printing speed, hatch spacing and extrusion width

for PolyMide™ CoPA and Polymax™ PC polymeric materials. The analysis was undertaken using the Taguchi method (a modelling strategy embedded into the software) to optimise and determine the parameters with the most significant impact. The larger is better feature was considered in this analysis, as recommended by Atakok *et al.* (2022). Table 7 presents data on the degree of fusion for specimens printed using different process parameters.

4.3.1 Bond formation and degree of fusion of filament-parts printed using PolyMide™ CoPA

Table 8 summarises the average values of the degree of fusion of PolyMide™ CoPA for different levels of layer thickness, printing speed, hatch spacing, extrusion temperature and extrusion width. Table 8 also ranks the significance of these process parameters based on the degree of fusion of two adjacent filaments.

The order of the significance of the selected process parameters, for PolyMide™ CoPA, in the foregoing table in order of the most to the least critical is as follows: extrusion temperature, layer thickness, extrusion width, hatch spacing and printing speed.

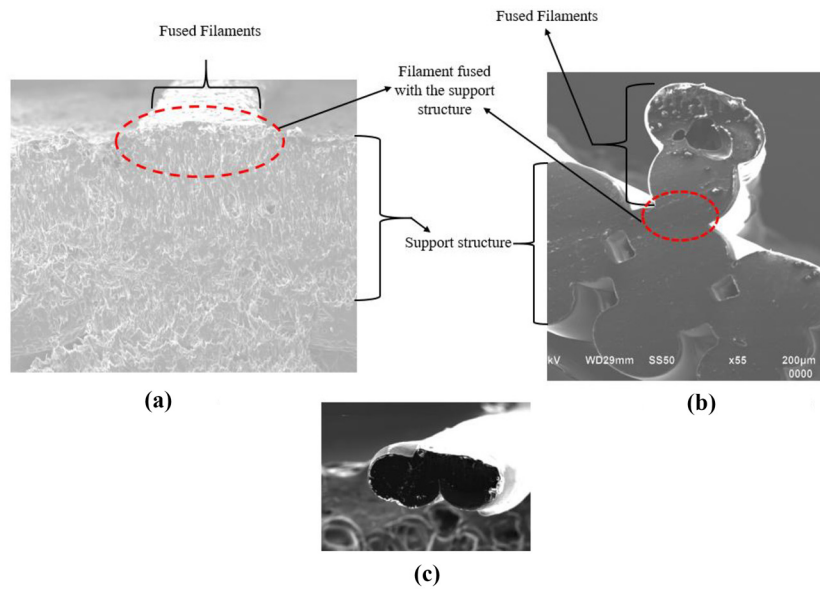
Figure 13 is a representation of plots for the mean values of the degree of fusion for adjacent filaments printed using PolyMide™ CoPA for the selected process parameters.

The values of process parameters corresponding to the highest degree of fusion were considered as the optimal process parameters. From Figure 13, the optimum process parameters for filaments printed using PolyMide™ CoPA are 0.25 mm, 40 mm/s, -0.10 mm, 255°C and 0.50 mm for layer thickness, printing speed, hatch spacing, extrusion temperature and extrusion width, respectively.

4.3.2 Bond formation and degree of fusion of filament-parts printed using Polymax™ PC

Table 9 outlines the average values of the degree of fusion of Polymax™ PC for different levels of layer thickness, printing

Figure 12 Cross-sectional view of tracks printed using PolyMide™ PA6-CF, PolyMide™ CoPA, and Polymax™ PC



Notes: (a) Cross-sectional of tracks printed using PolyMide™ PA6-CF (b) cross-sectional view of tracks printed using PolyMide™ CoPA; (c) cross-sectional of tracks printed using Polymax™ PC

Source: Figure by authors

speed, hatch spacing, extrusion temperature and extrusion width. Table 9 also ranks the significance of these process parameters based on the degree of fusion of two adjacent filaments.

The order of the significance of the selected process parameters, for Polymax™ PC, in the foregoing table in order of the most to the least critical is as follows: hatch spacing, extrusion width, layer thickness, printing speed and extrusion temperature.

The plots for the mean values of the degree of fusion for adjacent filaments printed using Polymax™ PC is as shown in Figure 14.

The optimal process parameters for Polymax™ PC, that would yield the highest degree of fusion of adjacent filaments, are 0.30 mm, 40 mm/s, 0.00 mm, 260°C and 0.6 mm for layer thickness, printing speed, hatch spacing, extrusion temperature and extrusion width respectively.

Table 7 Degree of fusion for tracks printed using PolyMide™ CoPA and Polymax™ PC at different process parameters

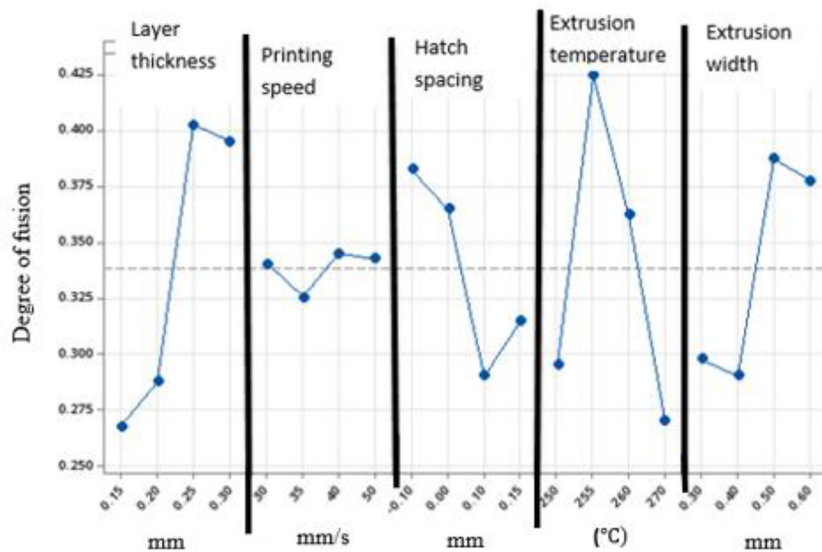
Run#	Layer thickness (mm)	Printing speed (mm/s)	Hatch spacing (mm)	Extrusion temperature (°C)	Extrusion width (mm)	Degree of fusion for tracks printed using PolyMide™ CoPA	Degree of fusion for tracks printed using Polymax™ PC
1	0.15	30	-0.10	250	0.30	0.23	0.22
2	0.15	35	0.00	255	0.40	0.32	0.21
3	0.15	40	0.10	260	0.50	0.30	0.26
4	0.15	50	0.15	270	0.60	0.22	0.31
5	0.20	30	0.00	260	0.60	0.38	0.41
6	0.20	35	-0.10	270	0.50	0.30	0.27
7	0.20	40	0.15	250	0.40	0.18	0.15
8	0.20	50	0.10	255	0.35	0.29	0.00
9	0.25	30	0.10	270	0.40	0.24	0.00
10	0.25	35	0.15	260	0.38	0.35	0.23
11	0.25	40	-0.10	255	0.60	0.58	0.44
12	0.25	50	0.00	250	0.50	0.44	0.34
13	0.30	30	0.15	255	0.50	0.51	0.48
14	0.30	35	0.10	250	0.60	0.33	0.20
15	0.30	40	0.00	270	0.40	0.32	0.35
16	0.30	50	-0.10	260	0.40	0.42	0.24

Source: Table by authors

Table 8 Levels and corresponding average values of process parameters used for PolyMide™ CoPA

Levels	Layer thickness (mm)	Average values of the degree of fusion after analysis			
		Printing speed (mm/s)	Hatch spacing (mm)	Extrusion temperature (°C)	Extrusion width (mm)
1	0.27	0.34	0.38	0.30	0.30
2	0.29	0.33	0.37	0.43	0.29
3	0.40	0.35	0.29	0.36	0.39
4	0.40	0.34	0.32	0.27	0.38
Rank	2	5	4	1	3

Source: Table by authors

Figure 13 Plots for mean values of degree of fusion for adjacent filaments printed using PolyMide™ CoPA

Source: Figure by authors

Table 9 Levels and corresponding average values of degree of fusion for five process parameters used for Polymax™ PC

Level	Layer thickness (mm)	Average values of the degree of fusion after analysis			
		Printing speed (mm/s)	Hatch spacing (mm)	Extrusion temperature (°C)	Extrusion width (mm)
1	0.25	0.28	0.29	0.23	0.20
2	0.21	0.23	0.33	0.28	0.15
3	0.25	0.30	0.12	0.29	0.34
4	0.32	0.22	0.29	0.23	0.34
Delta	0.11	0.08	0.21	0.06	0.19
Rank	3	4	1	5	2

Source: Table by authors

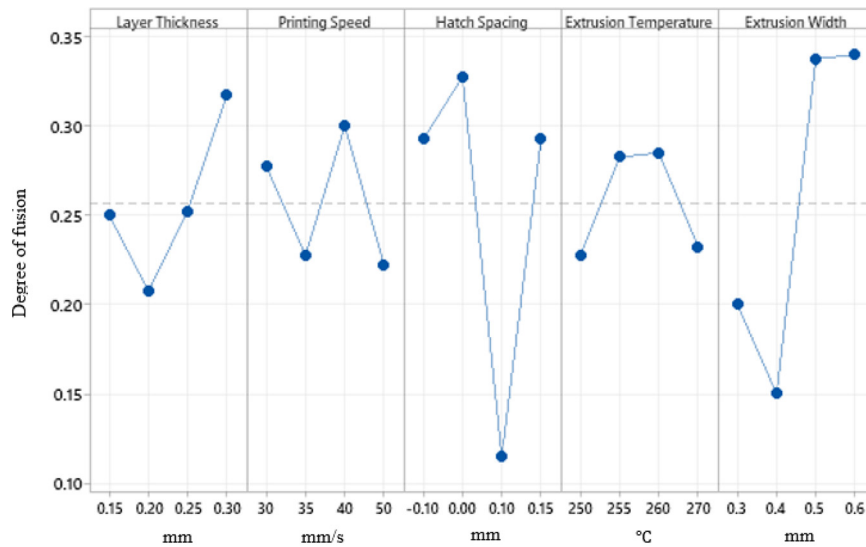
4.3.3 Linear regression models

Equations (8) and (9) are linear regression models that were developed in the present work using the regression module embedded in the Minitab Software. They show the relationship between the degree of fusion between two adjacent filaments with different process parameters (layer thickness, printing speed, hatch spacing, extrusion temperature and extrusion width) for PolyMide™ CoPA and Polymax™ PC, respectively. The models can be used to predict the optimal process parameters for the two

materials or other closely related polymers based on the degree of fusion between two adjacent filaments:

$$\delta_f (\text{PolyMide}^{\text{TM}} \text{CoPA}) = 0.769 + 0.995t + 0.00041s - 0.345h - 0.00313T + 0.338w \quad (8)$$

$$\delta_f \text{Polymax}^{\text{TM}} \text{PC} = 0.05 + 0.495t - 0.00184s - 0.336h - 0.00036T + 0.608w \quad (9)$$

Figure 14 Plots for the mean values of degree of fusion for adjacent filaments printed using Polymax™ PC

Source: Figure by authors

Table 10 Degree of fusion between two adjacent filaments printed using PolyMide™ CoPA and Polymax™ PC based on the experimental data and the proposed linear regression models

Run#	Degree of fusion for tracks printed using PolyMide™ CoPA (based on the experimental results)	Degree of fusion for tracks printed using PolyMide™ CoPA (Based on the linear regression model results)	% difference between experimental and linear regression model results (%)	Degree of fusion for tracks printed using Polymax™ PC (based on the experimental results)	Degree of fusion for tracks printed using Polymax™ PC (based on the linear regression model results)	% difference between experimental and linear regression model results (%)
1	0.23	0.28	21.74	0.22	0.20	09.09
2	0.32	0.27	15.63	0.21	0.21	0.00
3	0.30	0.26	13.33	0.26	0.23	11.53
4	0.22	0.24	09.09	0.31	0.25	19.35
5	0.38	0.37	02.63	0.41	0.37	09.76
6	0.30	0.34	13.33	0.27	0.33	22.22
7	0.24	0.29	20.83	0.15	0.18	20.00
8	0.29	0.26	10.34	0.00	0.14	14.00
9	0.24	0.29	20.83	0.00	0.23	23.00
10	0.35	0.27	22.86	0.23	0.20	13.04
11	0.58	0.47	18.97	0.44	0.40	09.09
12	0.44	0.42	04.55	0.34	0.30	11.76
13	0.51	0.40	21.57	0.48	0.31	35.42
14	0.33	0.47	42.42	0.25	0.38	27.57
15	0.32	0.34	06.25	0.35	0.27	22.86
16	0.42	0.44	4.76	0.24	0.29	20.83
			Overall (mean) difference = 15.57			Overall (mean) difference = 16.85

Source: Table by authors

where,

- δ_f = degree of fusion;
- t = layer thickness (m);
- s = sprinting speed (mm/s);
- h = hatch spacing (m);
- T = extrusion temperature ($^{\circ}C$); and
- w = extrusion width (m).

Table 10 compares the values of degree of fusion between two adjacent filaments printed using PolyMide™ CoPA and Polymax™ PC, based on the experimental data and calculated using equations (8) and (9), respectively.

The use of equation (8) on PolyMide™ CoPA resulted in an average difference in the degree of fusion of 15.57% between experimental and linear regression model. Similarly, applying

equation (9) to PolymaxTM PC, led to an average difference in the degrees of fusion of 16.85%. Clearly, the two respective linear regression models can be used to predict the degree of fusion between two adjacent filaments printed using PolyMideTM CoPA and PolymaxTM PC, noting the determined percentage differences.

5. Conclusions and recommendations

This study was conducted to investigate the surface and geometry of tracks printed using PolyMideTM CoPA, PolymaxTM PC and PolyMideTM PA6-CF. The study also examined the degree of fusion of adjacent filaments for PolyMideTM CoPA and PolymaxTM PC, to determine the optimal process parameters that would yield the highest degree of fusion between two adjacent filaments. The following conclusions can be drawn from the results presented and discussed here:

- PolyMideTM PA6-CF is most likely to present challenges when used in the FDM process to fabricate components as it was difficult to separate printed tracks from the support structure. The tracks also had noticeable surface irregularities that might limit the applications of final components due to the high probability of building parts with rough surfaces.
- Moderate irregularities were observed on the surfaces of tracks printed using PolyMideTM CoPA. Post-process operations such as cutting and grinding might be required to remove components that have been fabricated using this material from the support structure as there was some level of fusion between the printed tracks and the support structures.
- PolymaxTM PC might be considered the most suitable material, of all the three materials considered, for use in FDM here, because the printed tracks showed the smoothest surface, and it was easy to remove them from the support structures.
- The study results suggested the optimal process parameters for PolyMideTM CoPA as 0.25 mm, 40 mm/s, -0.10 mm, 255°C and 0.50 mm for layer thickness, printing speed, hatch spacing, extrusion temperature and extrusion width, respectively.
- The analysis carried out here came up with optimal process parameters for PolymaxTM PC of 0.30 mm, 40 mm/s, 0.00 mm, 260°C and 0.6 mm for layer thickness, printing speed, hatch spacing, extrusion temperature and extrusion width, respectively.

It is suggested that three dimensional samples be fabricated using the materials considered in this analysis to ascertain their utility in FDM. An evaluation should also be undertaken to examine the physical and mechanical properties of printed samples. Moreover, the influence of other process parameters (bed temperature, feed rate, printing time) on bond formation should also be investigated.

References

Ahmad, N.N., Wong, Y.H. and Ghazali, N.N.N. (2022), “A systematic review of fused deposition modeling process parameters”, *Soft Science*, Vol. 2 No. 11, pp. 1-35.

Alsoufi, M.S. and Elsayed, A.E. (2018), “Surface roughness quality and dimensional accuracy – a comprehensive analysis

of 100% infill printed parts fabricated by a personal/desktop cost-effective FDM 3D printer”, *Materials Sciences and Applications*, Vol. 9 No. 1, pp. 1–11.

Atakok, G., Kam, M. and Koc, H.B. (2022), “Tensile, three-point bending and impact strength of 3D printed parts using PLA and recycled PLA filaments: a statistical investigation”, *Journal of Materials Research and Technology*, Vol. 18, pp. 1542-1554.

Bhalodi, D., Zalavadiya, K. and Gurralla, P.K. (2019), “Influence of temperature on polymer parts manufactured by fused deposition modeling process”, *Journal of the Brazilian Society of Mechanical Sciences and Engineering*, Vol. 41 No. 3, pp. 1-11.

Bintara, R.D., Lubis, D.Z. and Pradana, Y.R.A. (2021), “The effect of layer height on the surface roughness in 3D printed polylactic acid (PLA) using FDM 3D printing”, *IOP Conference Series: Materials Science and Engineering*, Vol. 1034 No. 1, p. 12096.

Boschetto, A., Bottini, L. and Veniali, F. (2016), “Integration of FDM surface quality modeling with process design”, *Additive Manufacturing*, Vol. 12, pp. 334-344.

Dey, A. and Yodo, N. (2019), “A systematic survey of FDM process parameter optimization and their influence on part characteristics”, *Journal of Manufacturing and Materials Processing*, Vol. 3 No. 3, pp. 64-94.

Frenkel, J.A. (1945), “Viscous flow of crystalline bodies under the action of surface tension”, *J. Phys. (USSR)*, Vol. 9 No. 5, pp. 385-401.

Gao, X., Qi, S., Kuang, X., Su, Y., Li, J. and Wang, D. (2021), “Fused filament fabrication of polymer materials: a review of interlayer bond”, *Additive Manufacturing*, Vol. 37, p. 101658.

Gurralla, P.K. and Regalla, S.P. (2014), “Part strength evolution with bonding between filaments in fused deposition modelling: this paper studies how coalescence of filaments contributes to the strength of final FDM part”, *Virtual and Physical Prototyping*, Vol. 9 No. 3, pp. 141-149.

Han, W., Kong, L. and Xu, M. (2022), “Advances in selective laser sintering of polymers”, *International Journal of Extreme Manufacturing*, Vol. 4 No. 4, pp. 1-38.

Ismail, K.I., Yap, T.C. and Ahmed, R. (2022), “3D-printed fiber-reinforced polymer composites by fused deposition modelling (FDM): fiber length and fiber implementation techniques”, *Polymers*, Vol. 14 No. 21, pp. 4659-4695.

Joseph, T.M., Kallingal, A., Suresh, A.M., Mahapatra, D.K., Hasanin, M.S., Haponiuk, J. and Thomas, S. (2023), “3D printing of polylactic acid: recent advances and opportunities”, *The International Journal of Advanced Manufacturing Technology*, Vol. 125 Nos 3/4, pp. 1015-1035.

Krajangsawadi, N., Blok, L.G., Hamerton, I., Longana, M.L., Woods, B.K. and Ivanov, D.S. (2021), “Fused deposition modelling of fibre reinforced polymer composites: a parametric review”, *Journal of Composites Science*, Vol. 5 No. 1, pp. 1-38.

Kristiawan, R.B., Imaduddin, F., Ariawan, D., Ubaidillah and Arifin, Z. (2021), “A review on the fused deposition modeling (FDM) 3D printing: filament processing, materials, and printing parameters”, *Open Engineering*, Vol. 11 No. 1, pp. 639-649.

Li, L., Sun, Q., Bellehumeur, C. and Gu, P. (2002), “Investigation of bond formation in FDM process”, 2002

- International Solid Freeform Fabrication Symposium*, held at the University of TX in Austin on August 5-7.
- Lupone, F., Padovano, E., Casamento, F. and Badini, C. (2021), "Process phenomena and material properties in selective laser sintering of polymers: a review", *Materials*, Vol. 15 No. 1, pp. 183-220.
- Mwema, F.M. and Akinlabi, E.T. (2020), "Basics of fused deposition modelling (FDM)", *Fused Deposition Modeling: strategies for Quality Enhancement*, Springer International Publishing, Switzerland, pp. 1-15.
- Mwanja, F.M., Maringa, M. and Nsengimana, J. (2023), "Investigating the effect of process parameters on the degree of fusion of two adjacent tracks produced through fused deposition modelling of acrylonitrile butadiene styrene", *Polymer Testing*, Vol. 121, pp. 107981-107996.
- Naveed, N. (2021), "Investigate the effects of process parameters on material properties and microstructural changes of 3D-printed specimens using fused deposition modelling (FDM)", *Materials Technology*, Vol. 36 No. 5, pp. 317-330.
- Patel, R., Desai, C., Kushwah, S. and Mangrola, M.H. (2022), "A review article on FDM process parameters in 3D printing for composite materials", *Materials Today: Proceedings*, Vol. 60, pp. 2162-2166.
- Sukindar, N.A., Yasir, A.S.H.M., Azhar, M.D., Azhar, M.A.M., Abd Halim, N.F.H., Sulaiman, M.H., Sabli, A.S.H.A. and Ariffin, M.K.A.M. (2024), "Evaluation of the surface roughness and dimensional accuracy of low-cost 3D-printed parts made of PLA – aluminum", *Heliyon*, Vol. 10 No. 4, pp. 1-13.
- Syrylybayev, D., Zharylkassyn, B., Seisekulova, A., Akhmetov, M., Perveen, A. and Talamona, D. (2021), "Optimisation of

- strength properties of FDM printed parts – a critical review", *Polymers*, Vol. 13 No. 10, pp. 1587-1622.
- Tao, Y., Kong, F., Li, Z., Zhang, J., Zhao, X., Yin, Q., Xing, D. and Li, P. (2021), "A review on voids of 3D printed parts by fused filament fabrication", *Journal of Materials Research and Technology*, Vol. 15, pp. 4860-4879.
- Vanaei, H.R., Shirinbayan, M., Deligant, M., Khelladi, S. and Tcharkhtchi, A. (2021), "In-process monitoring of temperature evolution during fused filament fabrication: a journey from numerical to experimental approaches", *Thermo*, Vol. 1 No. 3, pp. 332-360.
- Xia, H., Lu, J. and Tryggvason, G. (2019), "A numerical study of the effect of viscoelastic stresses in fused filament fabrication", *Computer Methods in Applied Mechanics and Engineering*, Vol. 346, pp. 242-259.
- Xia, Q., Sun, G., Kim, J. and Li, Y. (2023), "Multi-scale modeling and simulation of additive manufacturing based on fused deposition technique", *Physics of Fluids*, Vol. 35 No. 3, pp. 1-13.

Futher reading

- Bellehumeur, C., Li, L., Sun, Q. and Gu, P. (2004), "Modeling of bond formation between polymer filaments in the fused deposition modeling process", *Journal of Manufacturing Processes*, Vol. 6 No. 2, pp. 170-178.

Corresponding author

Fredrick Mwanja can be contacted at: fredmulinge@gmail.com